



Metformin inhibits the pathogenic functions of AChR-specific B and Th17 cells by targeting miR-146a

Yue Hao^{a,1}, Wei Zhao^{a,1}, Lulu Chang^{a,1}, Xingfan Chen^a, Chonghui Liu^a, Yang Liu^a,
Lixuan Hou^a, Yinchun Su^a, Hao Xu^a, Yu Guo^a, Qixu Sun^c, Lili Mu^a, Jinghua Wang^a, Hulun Li^a,
Junwei Han^{b,*}, Qingfei Kong^{a,*}

^a Department of Neurobiology, Harbin Medical University, Heilongjiang Provincial Key Laboratory of Neurobiology, Harbin, Heilongjiang 150086, China

^b College of Bioinformatics Science and Technology, Harbin Medical University, Harbin, Heilongjiang 150081, China

^c YanTai PengLai, People's Hospital Digestive System Department, YanTai, ShanDong 265600, China

ARTICLE INFO

Keywords:

miR-146a
EAMG
T cells, B cells
Metformin

ABSTRACT

Myasthenia gravis (MG) is characterized by fatigable skeletal muscle weakness with a fluctuating and unpredictable disease course and is caused by circulating autoantibodies and pathological T helper cells. Regulation of B-cell function and the T-cell network may be a potential therapeutic strategy for MG. MicroRNAs (miRNAs) have emerged as potential biomarkers in immune disorders due to their critical roles in various immune cells and multiple inflammatory diseases. Aberrant miR-146a signal activation has been reported in autoimmune diseases, but a detailed exploration of the relationship between miR-146a and MG is still necessary. Using an experimental autoimmune myasthenia gravis (EAMG) rat model, we observed that miR-146a was highly expressed in the spleen but expressed at low levels in the thymus and lymph nodes in EAMG rats. Additionally, miR-146a expression in T and B cells was also quite different. EAMG-specific Th17 and Treg cells had lower miR-146a levels, while EAMG-specific B cells had higher miR-146a levels, indicating that targeted intervention against miR-146a might have diametrically opposite effects. Metformin, a drug that was recently demonstrated to alleviate EAMG, may rescue the functions of both Th17 cells and B cells by reversing the expression of miR-146a. We also investigated the downstream target genes of miR-146a in both T and B cells using bioinformatics screening and qPCR. Taken together, our study identifies a complex role of miR-146a in the EAMG rat model, suggesting that more caution should be paid in targeting miR-146a for the treatment of MG.

Abbreviations

MG	myasthenia gravis
EAMG	experimental auto-immune myasthenia gravis
AChR	anti-acetylcholine receptor
Th	T helper
miR-146a	microRNA-146a
α-BTX	alpha-bungarotoxin
NMJ	neuromuscular junction
LPS	lipopolysaccharide
SLE	systemic lupus erythematosus
RA	rheumatoid arthritis
MS	multiple sclerosis

1. Introduction

Myasthenia gravis (MG) is a neuroimmune disease mediated directly by B cells and their autoantibody secretions [1]. Clinically, skeletal muscle weakness and fatigue are the main symptoms of the disease, and serological tests show that approximately 70% of MG patients are positive for anti-acetylcholine receptor (AChR) antibodies. Anti-AChR antibodies, secreted by self-reactive B cells, attack AChR at neuromuscular junctions, leading to a decrease in the number of postsynaptic membranes AChR, the widening of the synaptic space and a decrease in folds or shallower sulci. As a consequence of AChR damage, the transmission of nerve electrical signals is then interrupted, resulting in muscle contraction disorders [2, 3]. It has been previously shown that without the presence of T helper (Th) cells, B cells alone could not induce MG

* Corresponding authors.

E-mail addresses: hanjunwei1981@163.com (J. Han), kqfangel@hrbmu.edu.cn (Q. Kong).

¹ These authors share first authorship

<https://doi.org/10.1016/j.imllet.2022.09.002>

Received 25 March 2022; Received in revised form 6 September 2022; Accepted 11 September 2022

Available online 13 September 2022

0165-2478/© 2022 European Federation of Immunological Societies. Published by Elsevier B.V. All rights reserved.

disease, since B-cell activation and antibody secretion depend on the assistance of T cells that recognize the same antigen [4–6].

Therefore, T helper cells play a vital role in MG disease. For example, the elevation of Th17 cells and their transcription factors, as well as their cytokines (IL-17A), have been detected in patients as well as animal models (experimental autoimmune myasthenia gravis, EAMG) of MG disease, whereas the function of Treg cells was attenuated, suggesting the important role of Th cells in the onset and development of MG diseases [7, 8]. IL-17 gene knockout mice have decreased levels of serum anti-AChR antibodies and complement binding antibodies, supporting the necessity of Th17-cell assistance for antibody secretion by B cells [9]. Understanding the molecular control of Th17 differentiation is likely the key to preventing pathogenic MG development. As a suppressor of Th17 cells, Treg cells are functionally deficient in MG patients. Although the number of CD4⁺CD25⁺ cells in the thymus of MG patients is normal when compared with that of healthy subjects, the mRNA and protein levels of the transcription factor Foxp3 and the cytokine IL-10 are significantly decreased, showing a weakness in their regulatory activity. Previous studies have also shown that the transfer of healthy rat Treg cells into myasthenia rats can prevent the occurrence of disease and alleviate EAMG disease development [10, 11]. These discoveries provide critical insights into the molecular factors that affect the differentiation and function of T cells and may participate in the progression of MG.

MicroRNAs (miRNAs) are a class of single-stranded endogenous noncoding RNAs with a size of 21 to 25 nucleotides. They are widely involved in different cell processes through posttranscriptional inhibition [12]. In particular, miR-146a has been identified as a vital regulator of immune reactions, participating in cell proliferation, differentiation, and apoptosis and is involved in the pathogenesis of autoimmune diseases [13]. Previous studies have shown that in the experimental autoimmune demyelinating model, Th17-cell differentiation, together with its relative cytokine levels (IL-17, IL-6, and IL-21), is elevated in miR-146a gene knockout mice. Additionally, miR-146a can effectively inhibit Th17-cell differentiation and then inhibit the release of inflammatory factors and alleviate disease [14–17]. The Foxp3-microRNA-146a-NF- κ B axis has been utilized in precancerous treatment since Foxp3 knockout can significantly reduce miR-146a expression. Low levels of miR-146a result in reduced inhibition of TRAF6 and IRAK1, eventually leading to the upregulation and activation of NF- κ B and aggravation of cancer development [18]. These findings highlight miR-146a as a potent regulator of Th17 and Treg cells. MiR-146a plays pivotal roles in regulating the proliferation of immune cells and inhibiting inflammatory responses [19]. Although some studies have also shown that in EAMG models, the number of anti-AChR antibodies, plasma cells and memory B cells decreased after miR-146a knockout in B cells [20]. However, the expression and function of miR-146a on MG-specific T cells are still unknown, and the downstream target genes of miR-146a in disease-specific T and B cells remain to be explored. In this study, we explore these questions and provide evidence for the clinical treatment of myasthenia gravis by targeting miR-146a.

2. Materials and methods

2.1. Animals

Six- to eight-week-old female Lewis rats weighing from 140 g to 160 g were purchased from Vital River Laboratory Animal Co. Ltd. (Beijing, China). The study was conducted according to the principles outlined in Harbin Medical University's Guide for the Care and Use of Laboratory Animals published by the China National Institute of Health.

2.2. Induction and clinical assessment of EAMG

Lewis rats were randomly selected for either the complete Freund's adjuvant (CFA) group or the EAMG group and then immunized with the

same dose (200 μ L/rat) of immune emulsion at the root of the tail. The immune emulsion for each CFA rat consisted of 100 μ L of incomplete Freund's adjuvant (IFA, Sigma Aldrich, St Louis, MO), 2 mg Mycobacterium tuberculosis (TB, Difco, Detroit, MI) and 100 μ L of phosphate-buffered saline (PBS). The only difference in the immune emulsion between the CFA and EAMG groups was that the R-AChR₉₇₋₁₁₆ peptide (synthesized by AC Scientific, Inc. Xi'an, China; 50 μ g/rat) was dissolved in PBS prior to preparing the emulsion for the EAMG groups. All rats underwent a second immunization with the same dose of emulsion without TB on Day 30 after the first immunization. Animals were weighed and monitored for their body weight and clinical scores every other day. A standard clinical score criteria was used that ranged from 0 (asymptomatic) to 4 (death status). The criteria for each score were as follows: 0, no disease and normal muscle strength; 1, mildly decreased activity and body weight, weak grip; 2, weakness, fatigue, clinical signs before exercise (tremors, head down, hunched posture); 3, severe generalized weakness, no grip, moribund; 4, dead. Clinical scores with intermediate signs were scored as 0.5, 1.5, 2.5 or 3.5 [21, 22]. These results were recorded as an average of each animal at each time point.

2.3. Enzyme-linked immunosorbent assay (ELISA)

For AChR antibody detection, ELISA plates (Corning CoStar 96-well plates, eBioscience, San Diego, CA) were precoated with affinity-purified AChR₉₇₋₁₁₆ peptide (1 μ g/mL) in 100 μ L of coating buffer (pH 9.6) per well at 4 °C overnight. Plates were washed with washing buffer 4 times after removing the precoating liquid, followed by 2 h of incubation at room temperature (RT) with blocking buffer (10% foetal calf serum). Next, the plates were loaded and incubated with serum (1:5,000, 100 μ L) from CFA and EAMG rats at RT for 2 h. After washing, rabbit anti-rat IgG antibody (DAKO, USA, 1:2,000, 100 μ L) was added to each well for an additional 2 h of incubation. Then, horseradish peroxidase (HRP)-conjugated goat anti-rabbit IgG (IBB Life Science, 1:5,000 dilution, 100 μ L) was added (37 °C, 1 hour). Next, 100 μ L TMB substrate solution (Biolegend, San Diego, CA) was added to each well and incubated at RT in the dark for 10 min. Finally, the reactions were stopped by the addition of 50 μ L H₂SO₄ per well. Absorbance was read at 450 nm with a Bio-Rad microplate reader (Bio-Rad Laboratories, Inc. Hercules, CA), and the recorded optical density values are presented as the mean \pm standard deviation (SD).

2.4. Tissue sampling and immunostaining

Tissues, such as brain, heart, lung lobe, muscle, liver, thymus, draining lymph nodes and spleen, were collected from two groups of rats after anaesthetizing. A 75% amplitude ultrasound was performed in 500 μ L TRIzol to decompose each tissue for subsequent qPCR detection.

Alpha-bungarotoxin (α -BTX) is known to bind irreversibly and competitively to nicotinic acetylcholine receptors (AChRs) at the neuromuscular junction (NMJ), reflecting the number and density of AChRs at NMJs. To assess the loss and damage of AChRs, eyelid tissues were also immediately separated and cryoprotected in Tissue-Tek OCT Compound (Sakura, Japan) for α -BTX staining by immunofluorescence analysis. Ten-micrometer-thick frozen sections were prepared with cold acetone for 15 min, blocked in 5% normal foetal bovine serum and stained with α -BTX (Thermo Fisher, USA, 1:400 diluted in 5% foetal bovine serum) overnight at 4 °C. Finally, the sections were observed and imaged using an LSM700 confocal microscope (Carl Zeiss, Germany). Dense AChR clusters at the neuromuscular junction of eyelid tissue stained by α -BTX were marked in red.

2.5. Cell preparation

Mononuclear cells were harvested from the inguinal, popliteal, para-aortic lymph nodes and spleen of immunized animals with a clinical score of 2 or 3. Cells were gathered by passing cell suspensions through a

40 μm cell strainer. CD4^+ T cells and B220^+ B cells were subsequently isolated by performing a negative selection with a MagCelect Rat CD4^+ T-Cell Isolation Kit and a MagCelect Rat B-Cell Isolation Kit (R&D Systems, Inc., USA) according to the manufacturer's instructions. A total of 1×10^8 EAMG rat splenocytes were prepared for isolation, and $2 \times 10^7 - 3.5 \times 10^7$ CD4^+ T lymphocytes were collected after purification. These purified cells were then stimulated with 10 $\mu\text{g}/\text{mL}$ R-AChR_{97–116} in RPMI 1640 medium (Sigma–Aldrich) supplemented with 1% sodium pyruvate (Sigma, USA), 10% foetal bovine serum, 1% nonessential amino acids (Sigma, USA), 1% L-glutamine (Sigma–Aldrich), 1% penicillin–streptomycin (Gibco, Paisley, UK), and 2-mercaptoethanol (2-ME, Amresco, Solon, OH, USA) for 72 h of incubation *in vitro*, followed by flow cytometry staining as described in 2.7.

For the polarization assays, purified CD4^+ T-cell stimulation and polarization were performed *in vitro*. The CD4^+ T cells adjusted at a density of 1×10^7 cell/mL in 2 mL medium were cultured in a 12 flat bottom orifice precoated with both anti-CD3 (purified anti-rat CD3 antibody, Biolegend, San Diego, CA; 2 $\mu\text{g}/\text{mL}$) and anti-CD28 (purified anti-rat CD28 antibody, Biolegend, San Diego, CA; 2 $\mu\text{g}/\text{mL}$) antibodies. Consequently, Th17 and Treg cells were activated and polarized using TGF- β (2 ng/mL for Th17 cells and 5 ng/mL for Treg cells) with or without IL-6 (20 ng/mL) for 72 h of incubation. Polarized Th17 and Treg cells were identified and enriched by flow sorting. A total of $2 \times 10^6 - 4 \times 10^6$ cells of polarized Th17 and Treg cells were collected and prepared for the qPCR experiments.

2.6. Quantitative real-time PCR analysis (qPCR)

Total RNA was isolated from enriched CD4^+ T cells, B cells, Th17 cells and Treg cells with TRIzol reagent (Invitrogen) according to the manufacturer's instructions. Complementary cDNA was synthesized for each 1 μg microRNA (total RNA) sample with a miRNA reverse transcription kit (qRT–PCR Detection kit, Gene Copoiea), and a 7500 real-time qPCR system was used to perform semi-quantitative amplification. *U6* was selected as an internal control. The primer sequences (listed 5'-3') used in this study were as follows: *U6* forward: CTCGCTTCGGCAGCACA, reverse: AACGTT CACGAATTTGCGT. *rno-miR-146a-5P*: AGAACTGAATTCATGGGTTAA, *mmu-miR-146a-5P*: UGAGAACUGAAUUCUAGGGUU. *Irak1* forward: GACTTTGGTCTGGCTCGTTTCA, reverse: TCACTCCACCTCTTCAGCCT. *Hnnpd* forward: GGACACCA-CAAAGAAAGACCTG, reverse: CCTCACCAAAAACCACCAAAGTA. *Nova1* forward: CACAGCAGGTCTGATAATAGGG, reverse: CGCAA-CACCGCAAAGGT. *Btg2* forward: CGAGCAGAGACTCAAGGTTTTCA, reverse: ATAGCCGGAGCCCTTGA. *Traf6* forward: AGGTTACAA-TACGCCTCAG, reverse: GCTACACGCTGCATCAGTA. *Siah2* forward: AAGTTCGCTCGGCAGTT, reverse: GGACGGTATTACAGATGTCTTCA. *Brd4* forward: ACCAGTTCCTTGCATCCA, reverse: TCAGCCCTGCCCTTTACC. *Ppp1r11* forward: CGGAAACGGAAGCCA-GAG, reverse: CACCAAAGGCCGAGGT. *Dot1l* forward: CCTCGTCCAAGCAGAACACC, reverse: GGCACGCTCCTTTACACCCT. *Kdm2b* forward: TTCAAACGTCCCCGGTTC, reverse: CCAG-GACCGCCGCTTT. *Usp3* forward: GCAGGGAGGCGGACATA. reverse: GCTGAGCGGGAAACACC.

2.7. Flow cytometry

Nuclear transcription factors and cell surface markers were detected by flow cytometry. Cells were stimulated by brefeldin A (1:1,000 dilution), ionomycin (1 mg/ml), and PMA (50 ng/ml) for 4–6 h before collection. Briefly, cells were first incubated with anti-Rat-CD4-FITC-conjugated (Invitrogen), anti-Rat-CD45R(B220)-FITC-conjugated (Invitrogen), or anti-Mouse-CD19-FITC-conjugated (Invitrogen) antibodies for 30 min at 4 °C. Intracellular staining was then performed with anti-Rat-IL-17A-PE-conjugated (eBioscience) and anti-Rat-Foxp3-APC-conjugated (Invitrogen) antibodies. For viability detection, cells were stained with an Annexin V-FITC/PI kit (MULTI SCIENCES). Cells were

detected using a BD FACS Verse flow cytometer and analysed using FlowJo software.

2.8. CCK8 analysis

A total of 200 μL of 2×10^6 cells/mL of lymphocytes and spleen cells derived from EAMG rats were plated into 96-well plates with different concentrations of metformin or LPS and incubated for 48 h. After the incubation step, 10 μL of Cell Counting Kit-8 (CCK-8, Dojindo, Japan) reagent was added to the medium and then stimulated for an additional 4 h. The absorbance values were measured at 450 nm on an ELISA plate reader (Bio-Rad Laboratories, Inc. Hercules, CA).

2.9. Statistical analysis

All experiments were repeated three times or more. A Student's t test was performed for statistical comparisons between two groups, and single factor ANOVA was used for the data analysis of three groups using Prism 7 software (GraphPad, San Diego, CA). All data are shown as the mean \pm standard deviation. $P < 0.05$ is considered statistically significant (*, $P < 0.05$; **, $P < 0.01$; ***, $P < 0.001$).

3. Result

3.1. Establishment of the EAMG animal model

The female Lewis rats were randomly divided into a CFA control group and an EAMG experimental group. The immune emulsion was injected into the tail root on Days 0 and 30, and then the clinical score and weight were measured every other day. Compared with the normal CFA group, EAMG rats showed obvious myasthenia signs beginning on the 38th day after the first immunization, and symptoms worsened over time (Fig. 1 A, 38 d: * $P < 0.05$, 40–48 d: **** $P < 0.0001$). In addition, EAMG rats displayed significant weight loss beginning on the 40th day after the first immunization (Fig. 1 B, 40 d: * $P < 0.05$, 42–48 d: **** $P < 0.0001$). Data from the ELISAs showed clearly increased serum anti-AChR antibody levels in EAMG rats (Fig. 1 C, **** $P < 0.0001$). Further, the immunofluorescence labelling method for α -BTX staining was used to label AChR clusters at the NMJ of eyelid muscle. The results showed that the fluorescence intensity of α -BTX in the EAMG group was much weaker than that in the control group, with apparent intermittent morphology (Fig. 1 D), suggesting that the AChRs clustered at the NMJ of eyelid muscle were damaged and lost. The above results indicate that we successfully established the EAMG rat model, which we then used in subsequent experiments.

3.2. The detection of miR-146a expression in tissues

Different tissues of rats in both the EAMG and CFA groups, including the brain, heart, lung lobe, muscle, liver, thymus, draining lymph node and spleen, were collected and prepared for the detection of miR-146a expression by qPCR. The results showed that miR-146a expression was significantly different between these two groups only in immune organs, such as the thymus, lymph nodes and spleen. The levels of miR-146a in the thymus (Fig. 2, *** $P < 0.001$) and drainage lymph nodes (Fig. 2, ** $P < 0.01$) of EAMG rats were obviously decreased compared with those in the CFA control group. However, a higher level of miR-146a expression in splenic tissue of EAMG rats (Fig. 2, *** $P < 0.001$) was observed, indicating that miR-146a expression is tissue dependent. The thymus is the source of immature T cells, and drainage lymph nodes are also enriched by T cells, while the spleen is composed mainly of B cells. Thus, the lower levels of miR-146a in T cell-enriched immune tissues, and its elevated expression in the spleen suggest that differential expression of miR-146a may occur in T and B cells.

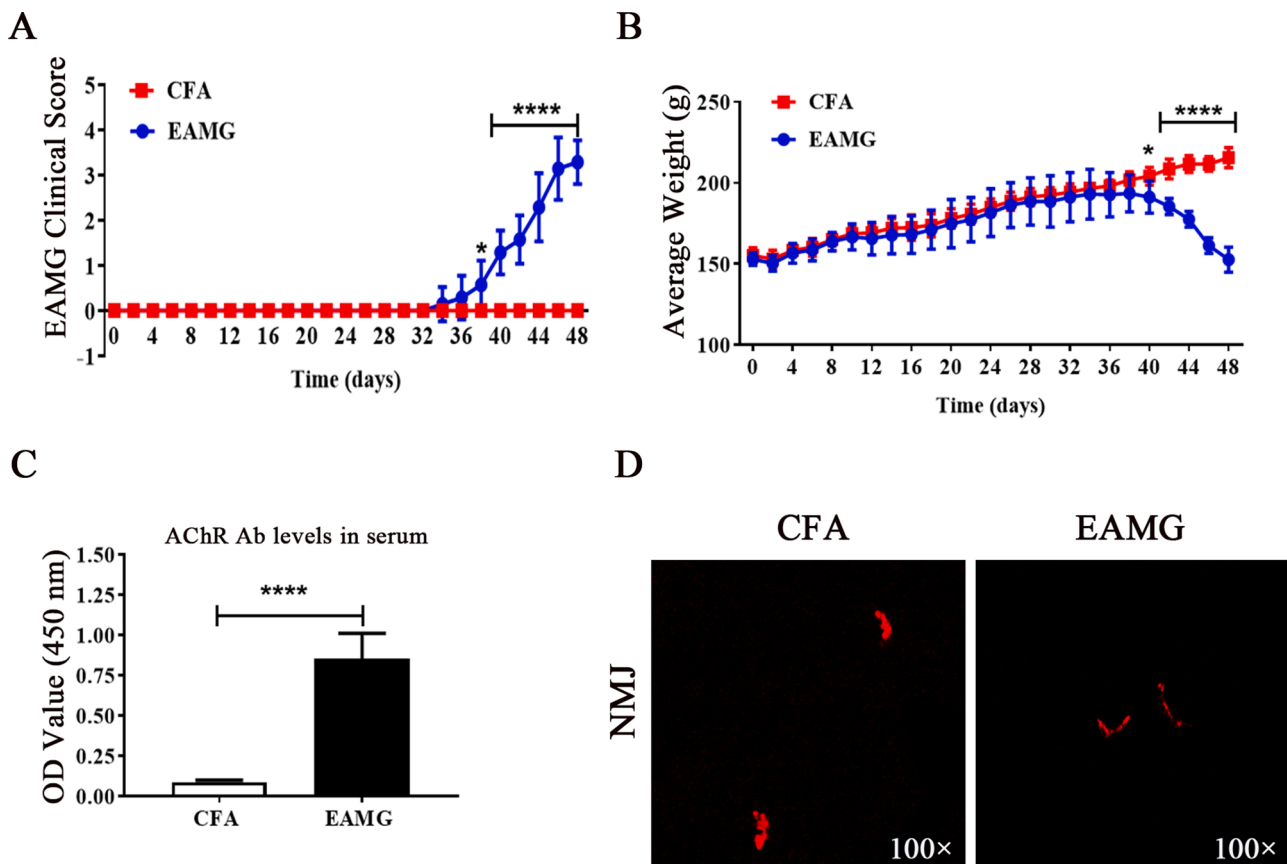


Fig. 1. Establishment of the EAMG rat model. (A) Clinical scores. (B) Body weight. (C) AChR-specific antibody levels in serum as measured using ELISA. (D) α -BTX staining. Data are presented as the mean \pm SD from 3 independent experiments with seven rats per condition per experiment, * $P < 0.05$, **** $P < 0.0001$, one-way ANOVA and t test ($n = 7$).

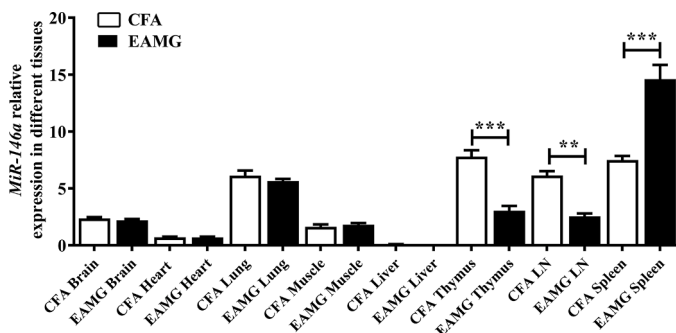


Fig. 2. The expression of miR-146a in different tissues or organs. Data are presented as the mean \pm SD from independent experiments with four rats per condition per experiment, ** $P < 0.01$, *** $P < 0.001$, one-way ANOVA ($n = 4$).

3.3. MiR-146a expression in AChR-specific T and B cells

To further investigate whether miR-146a expression in T and B cells is distinct, a single cell suspension from spleen tissues of rats was prepared for the purification of T and B cells via magnetic activated cell sorting. T cells (CD4⁺) with purity above 95% (Fig. 3 A) and B cells (CD45R⁺) with purity above 90% (Fig. 3 C) were then prepared for the detection of miR-146a expression by qPCR. Compared with the CFA control group, the miR-146a level in EAMG-specific T cells was obviously reduced (Fig. 3 B, *** $P < 0.001$), while the expression of miR-146a in B cells was markedly higher than that in the control group (Fig. 3 D, ** $P < 0.01$). Thus, miR-146a expression was decreased in AChR-specific T cells and increased in AChR-specific B cells.

Next, isolated T and B cells from the CFA and EAMG groups were incubated for 24 h *in vitro* with 10 μ g/mL AChR peptide stimulation, and the miR-146a expression levels were then analysed. Compared with the CFA group, the miR-146a levels in EAMG-specific T cells were significantly decreased regardless of whether the incubation time was 0 h or 24 h (Fig. 3 E, 0 h: * $P < 0.05$, 24 h: * $P < 0.05$). The expression of miR-146a in the B cells of EAMG rats was higher than that of the CFA group at both time points (Fig. 3 E, 0 h: ** $P < 0.01$, 24 h: * $P < 0.05$). MiR-146a expression in T and B cells was also cell dependent, which is consistent with our results in Fig. 2.

3.4. MiR-146a expression in Th17 and Treg cells

All of the above results indicate low expression of miR-146a in EAMG-specific T cells. Since T cells, especially the balance of Th17 and Treg cells, are closely related to the development of MG disease, the levels of miR-146a in both disease-specific Th17 and Treg cells should also be considered. Th17 and Treg cell polarizations were prepared under different polarizing conditions. Compared with that in the CFA healthy control group, the miR-146a expression in both EAMG-specific Th17 cells (Fig. 4 A, * $P < 0.01$) and EAMG-specific Treg cells (Fig. 4 B, ** $P < 0.01$) was clearly decreased in EAMG rats.

3.5. Determination of metformin treatment concentration

Increasing evidence suggests that metformin plays roles not only in the control of blood sugar but also in regulating inflammation [23, 24]. In type 2 diabetes, it has been reported that metformin can relieve symptoms by inhibiting the function of miR-146a [25, 26]. In addition, in our previous study we demonstrated that metformin alleviates disease

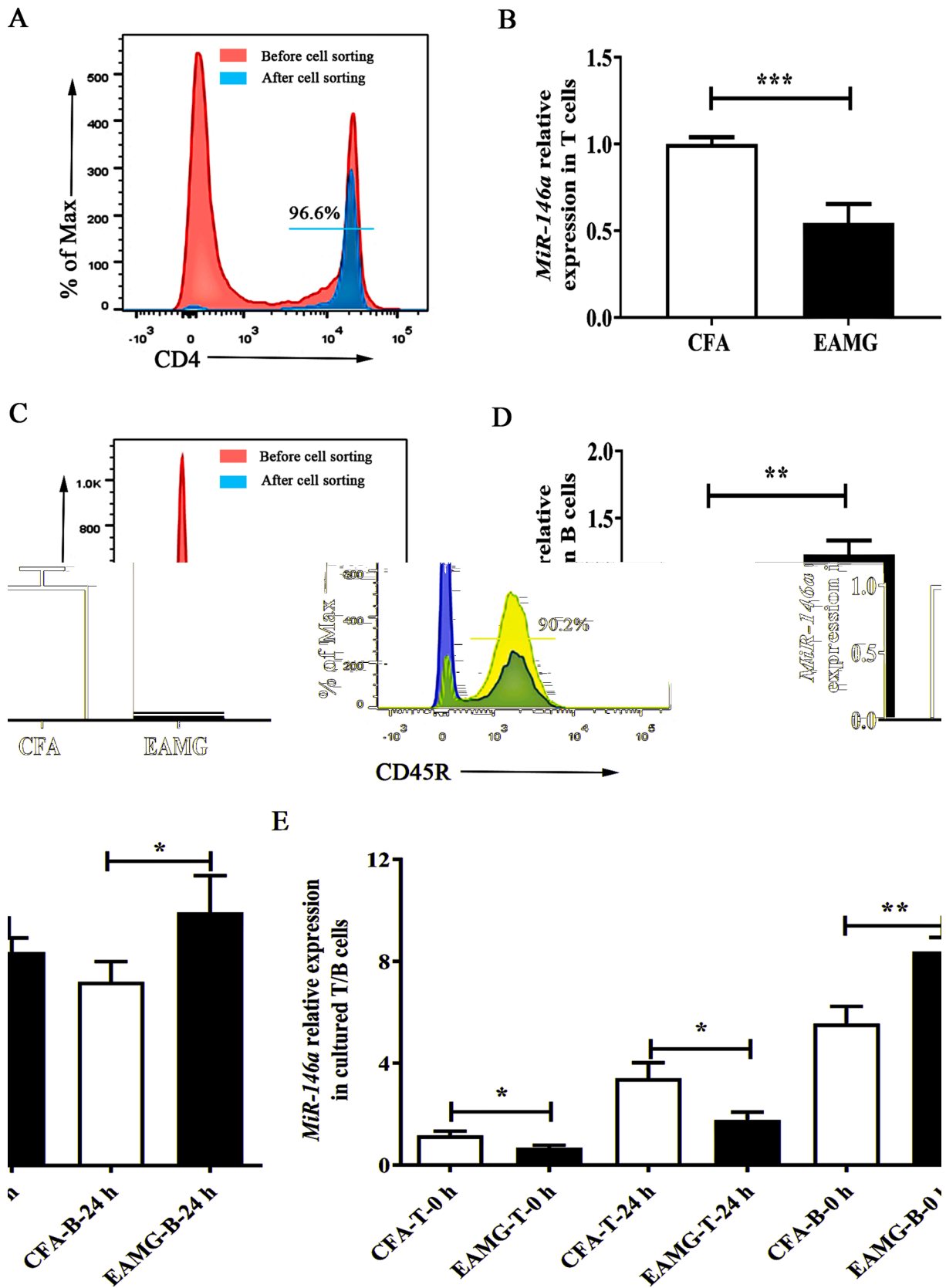


Fig. 3. Differential expression of miR-146a in T and B cells. The purity of T cells (A) and B cells (C) were detected by flow cytometry. The expression of miR-146a in T cells (B) and B cells (D) was measured using qPCR. (E) The expression of miR-146a in T cells and B cells *in vitro* with or without 24 h AChR stimulation. Data are presented as the mean \pm SD from three independent experiments with five rats per condition per experiment, * $P < 0.05$, ** $P < 0.01$, *** $P < 0.001$, *t* test, one-way ANOVA ($n = 5$).

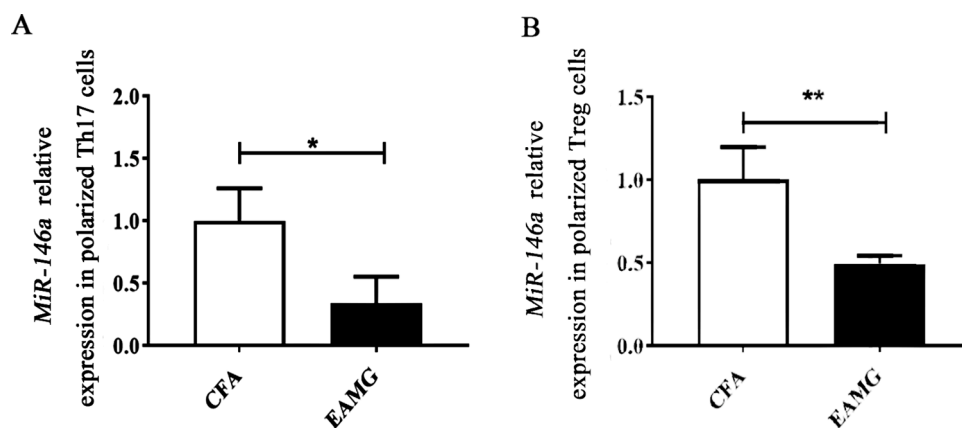


Fig. 4. The levels of miR-146a in T-cell subsets. (A) Expression of miR-146a in Th17 cells. (B) Expression of miR-146a in Tregs. Data are presented as the mean ± SD from two independent experiments with six rats per condition per experiment, * $P < 0.05$, ** $P < 0.01$, t test ($n = 6$).

by inhibiting EAMG-specific Th17-cell differentiation through the AMPK pathway. Clinical symptoms, serum antibody content and histopathological changes were significantly reversed after metformin drug intervention [27]. Therefore, we hypothesized that metformin could ameliorate EAMG disease by targeting miR-146a.

A single-cell suspension of EAMG lymphonodus was stimulated by AChR (10 µg/mL) with different concentrations of metformin (0, 0.5, 1, 2, 5, 10, 50, or 100 mM), followed by CCK-8 detection for the analysis of cell proliferation. The results showed that metformin, at concentrations of 0.5 mmol/L and 1 mmol/L, did not affect the proliferation of lymphocytes (Fig. 5 A, NS = no significant difference). However, when the concentrations were increased to 2 mmol/L or higher (5-100 mmol/L),

cell proliferation was clearly inhibited (Fig. 5 A, * $P < 0.05$, *** $P < 0.001$) compared with that of the nontreated group. Additionally, after incubation with metformin (0, 0.5, 1, or 2 mM) for 48 h, cell viability was detected by apoptosis staining of Annexin V-FITC and PI, and the miR-146a expression of these lymphocytes was then measured using qPCR and the supernatant was also collected for the detection of AChR antibody content. The data showed that metformin at concentrations of 0.5 mmol/L and 1 mmol/L did not affect the viability of lymphocytes, while 2 mmol/L metformin significantly increased the proportion of apoptotic cells (Fig.5 B-C, NS = no significant difference, ** $P < 0.01$). Since miR-146a expression in lymphocytes was only significantly induced by 0.5 mmol/L metformin (Fig. 5 D, * $P < 0.05$) and AChR

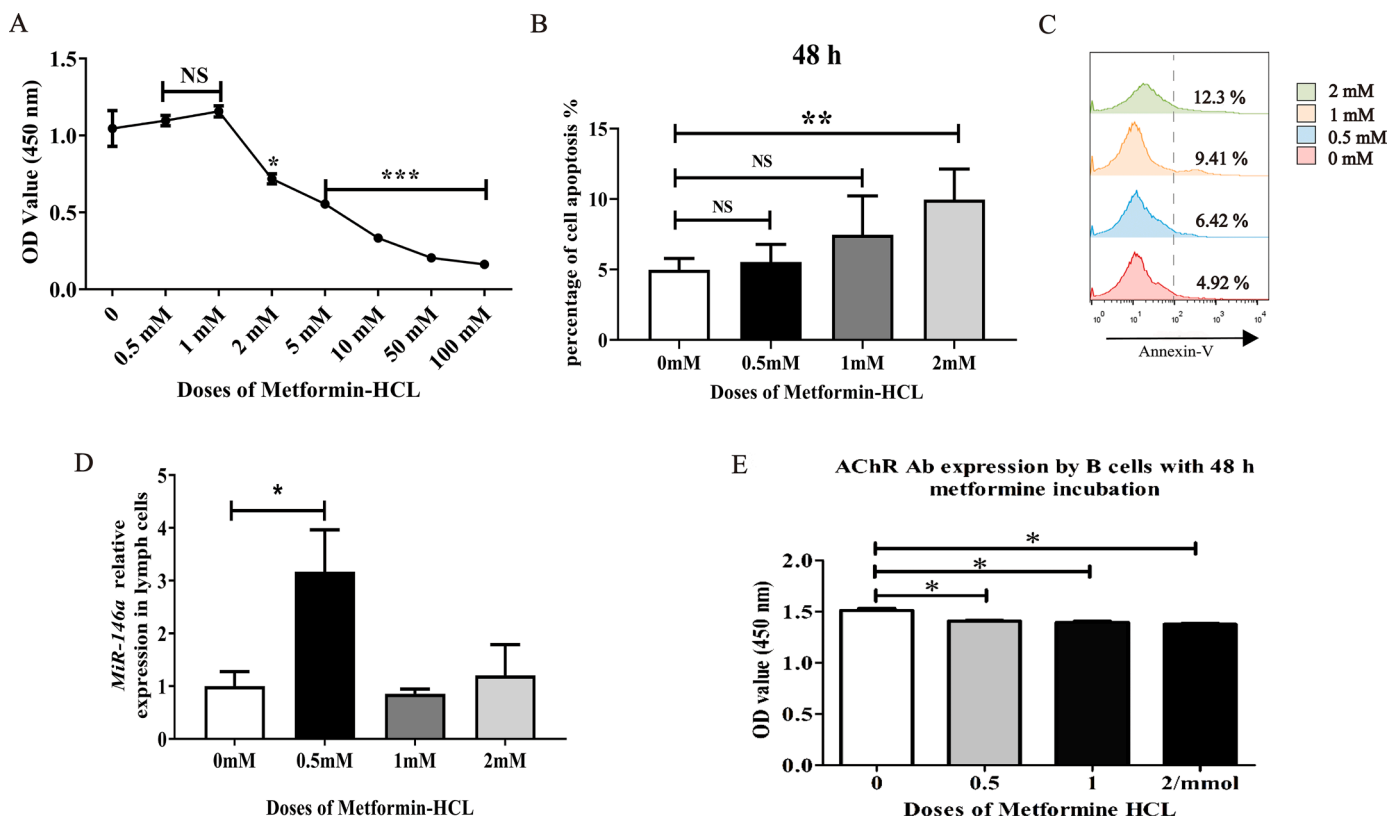


Fig. 5. Determining the concentration of metformin treatment *in vitro*. (A) Proliferation assay using a CCK8 kit after different doses of metformin incubation ($n = 3$). (B-C) Cell activity assay using an Annexin V-FITC/PI kit after different doses of metformin incubation ($n = 3$). (D) Expression of miR-146a in lymph node cells using qPCR ($n = 6$). (E) AChR-specific antibody levels in B cells by ELISA ($n = 5$). Data are presented as the mean ± SD from two independent experiments, NS = no significant difference, * $P < 0.05$, ** $P < 0.01$, *** $P < 0.001$ one-way ANOVA, t test.

antibody secretion was decreased by metformin at 0.5 mmol/L, 1 mmol/L and 2 mmol/L (Fig. 5 E, * $P < 0.05$), a metformin concentration of 0.5 mmol/L was selected for subsequent experiments due to its roles in decreasing antibody secretion while elevating miR-146a expression.

3.6. MiR-146a expression is affected by metformin in Th17 and Treg cells

The above experimental results showed that metformin at a concentration of 0.5 mmol/L upregulated the expression of miR-146a in lymphocytes. For further experiments, CD4⁺ positive cells from EAMG rats were polarized into Th17 and Treg cells with or without 0.5 mmol/L metformin and prepared for the analysis of miR-146a expression. Compared with the nontreated control, 0.5 mmol/L metformin clearly decreased the portion of CD4⁺IL-17⁺ double-positive cells (Fig. 6 A-B, ** $P < 0.01$), indicating an inhibitory effect of metformin on Th17 differentiation, while the miR-146a level in polarized Th17 cells was distinctly increased (Fig. 6 C, * $P < 0.05$). However, as shown in Fig. 6 D-E (NS = no significant difference), the addition of metformin had no significant effect on Treg cell polarization, which are characterized by CD4⁺Foxp3⁺, though the expression of miR-146a in Treg cells was statistically decreased after metformin incubation (Fig. 6 F, * $P < 0.05$). Although there was no change in the proportion of Treg cells, the reduction in Th17 cells could also cause a decrease in the Th17/Treg ratio and the Treg bias, which might be beneficial for the relief of MG disease. These results indicated that metformin, by targeting miR-146a, could decrease the Th17/Treg ratio and the Treg bias by inhibiting the differentiation of Th17 proinflammatory cells. However, the role of miR-146a in Tregs remains to be further explored.

3.7. LPS stimulation in vitro

A single cell suspension from CFA rats was prepared for lipopolysaccharide (LPS) stimulation *in vitro*. CCK8 proliferation experiments were performed after 48 h of incubation. A significant increase in cell proliferation was observed after the addition of 5 µg/mL LPS (Fig. 7 A, ** $P < 0.01$, *** $P < 0.001$). In addition, cell colony formation was also observed (Fig. 7 B-C), and the cell density and volume visibly increased to the naked eye (Fig. 7 D-E) following 5 µg/mL LPS stimulation. The arrowhead indicates that lymphocytes were significantly enlarged after 48 h of LPS stimulation (Fig. 7 E). The above results suggest that 5 µg/mL LPS can effectively stimulate lymphocyte activation.

3.8. The effects of metformin on miR-146a expression in B cells

A mixed single-cell suspension was activated with 0.5 µg/mL LPS for 48 h, followed by an additional incubation with or without 0.5 mmol/L metformin before flow cytometry detection. Metformin (0.5 mmol/L) showed a significant inhibitory effect on CD19⁺ B cells (Fig. 8 A-B, ** $P < 0.01$). In addition, 0.5 mmol/L metformin decreased the expression of miR-146a in activated CD19⁺ B cells compared with the nontreated group (Fig. 8 C, * $P < 0.05$). These data indicate that metformin might partially attenuate B-cell content by targeting miR-146a expression.

3.9. Prediction and verification of miR-146a downstream target genes

Three databases, TargetScan, miRDB and miRwalk, were used for the prediction of rno-miR-146a-5p downstream target genes. A total of 186, 211 and 5706 downstream target genes were collected from the above three different databases. As shown in Fig. 9 A, twenty predicted rno-miR-146a-5p downstream target genes simultaneously reported by all three databases were screened, including *Irak1*, *Slc10a3*, *Hnrnpd*, *Nova1*, *Usp3*, *Btg2*, *Traf6*, *Rarb*, *Bcor1*, *Siah2*, *Rfx7*, *Brd4*, *Ppp1r11*, *Dot1l*, *Fbxw2*, *Armc8*, *Zfyve1*, *Hic2*, *Pip5k1b* and *Kdm2b*. Among these genes, the *Irak1* [28, 29], *Hnrnpd* [30], *Nova1* [31], *Btg2* [32], *Traf6* [33, 34], *Siah2* [35], *Brd4* [36], *Ppp1r11* [37], *Dot1l* [38] and *Kdm2b* [39] genes are thought to be related to T-cell functions, while the *Irak1* [40], *Usp3* [41], *Traf6*

[42], *Siah2* [43], *Brd4* [44] and *Dot1l* [45] genes are thought to be related to B-cell function (Table 1).

For further analysis, purified EAMG-derived T and B cells pretreated with or without 0.5 mmol/L metformin were prepared for the detection of the expression of these predicted target genes by qPCR. As shown in Fig. 9 B-C, compared with the nontreated control, 0.5 mmol/L metformin clearly increased *Btg2* gene expression in T cells and *Brd4* gene expression in B cells, while it significantly decreased *Nova1* and *Brd4* gene expression in T cells and *Traf6* gene expression in B cells. However, the rest of the predicted genes were not significantly altered by metformin (Fig. 9 B-C, * $P < 0.05$, ** $P < 0.01$, NS = no significant difference). These results indicate that the screened target genes of miR-146a were indeed expressed in EAMG-derived T and B cells and that metformin could also affect miR-146a by targeting the *Btg2*, *Nova1* and *Brd4* genes in T cells, as well as the *Brd4* and *Traf6* genes in B cells.

4. Discussion

MicroRNA (miRNA), a class of single-stranded endogenous non-coding RNA with a size of 21 to 25 nucleotides, is widely involved in different cell processes through posttranscriptional inhibition [46]. Previous studies have reported an unusual expression of miR-146a in different types of immune cells and autoimmune diseases, and up- or downregulation of miR-146a expression has notable effects on immune cell functions, suggesting that miR-146a may be a therapeutic target in autoimmune diseases [47, 48]. However, the mechanism by which miR-146a participates in myasthenia gravis (MG) and its animal model, experimental autoimmune myasthenia gravis (EAMG), is still unknown. In this study, we demonstrate the complex role of miR-146a in myasthenia gravis disease.

MiR-146a has been reported to be a negative regulator of TLRs involved in inflammatory pathogenesis. The overexpression of miR-146a may inhibit the activation of inflammatory signals and secretion of proinflammatory cytokines in systemic lupus erythematosus (SLE) by targeting and regulating IRAK1 expression through the TLR-4/MYD88/NF-κB pathway [47]. Nevertheless, the expression of miR-146a in SLE patients with anaemia was significantly higher than that in healthy controls, unlike in typical SLE patients [49]. The expression level of miR-146a is also complex in rheumatoid arthritis (RA), as it is overexpressed in many tissues, such as the synovial membrane and cartilage, in patients with arthritis, and it is especially increased significantly in joint synovial CD4⁺ T cells [48, 50]. However, miR-146a is expressed at low levels in the Ly6C^{high} monocyte subgroup of RA patients, and artificial overexpression of miR-146a in this cell subgroup can effectively relieve joint damage and arthritis symptoms [51]. Therefore, miR-146a could be regarded as a biological marker or a potential therapeutic target for autoimmune diseases due to its differential expression in immune diseases and immune cells.

MG disease is characterized by AChR antibodies secreted by B cells [52]. B-cell activation depends on T-cell assistance [53] since the levels of serum AChR antibody are reduced in CD4⁺ T cells and CD8⁺ T-cell knockout EAMG mice [54], suggesting the pivotal roles of both T and B cells during MG disease progression. We observed different expression of miR-146a in distinct immune organs and immune cells in the EAMG model and showed for the first time that miR-146a was highly expressed in EAMG-specific spleen and B cells but expressed at lower levels in drainage lymph nodes, thymus and disease-specific T cells. In addition, we further observed significantly decreased levels of miR-146a in both EAMG-specific Th17 and Treg cells compared with those in cells of the CFA group. Based on these data, we hypothesized that the differential expression of miR-146a in immune cells may be associated with its diverse roles in B and T cells, so we investigated whether the regulation of miR-146a expression would reverse the pathogenic function of EAMG-specific B and T cells.

Recent studies have suggested that metformin is not only a hypoglycaemic agent but also widely researched for its impacts on

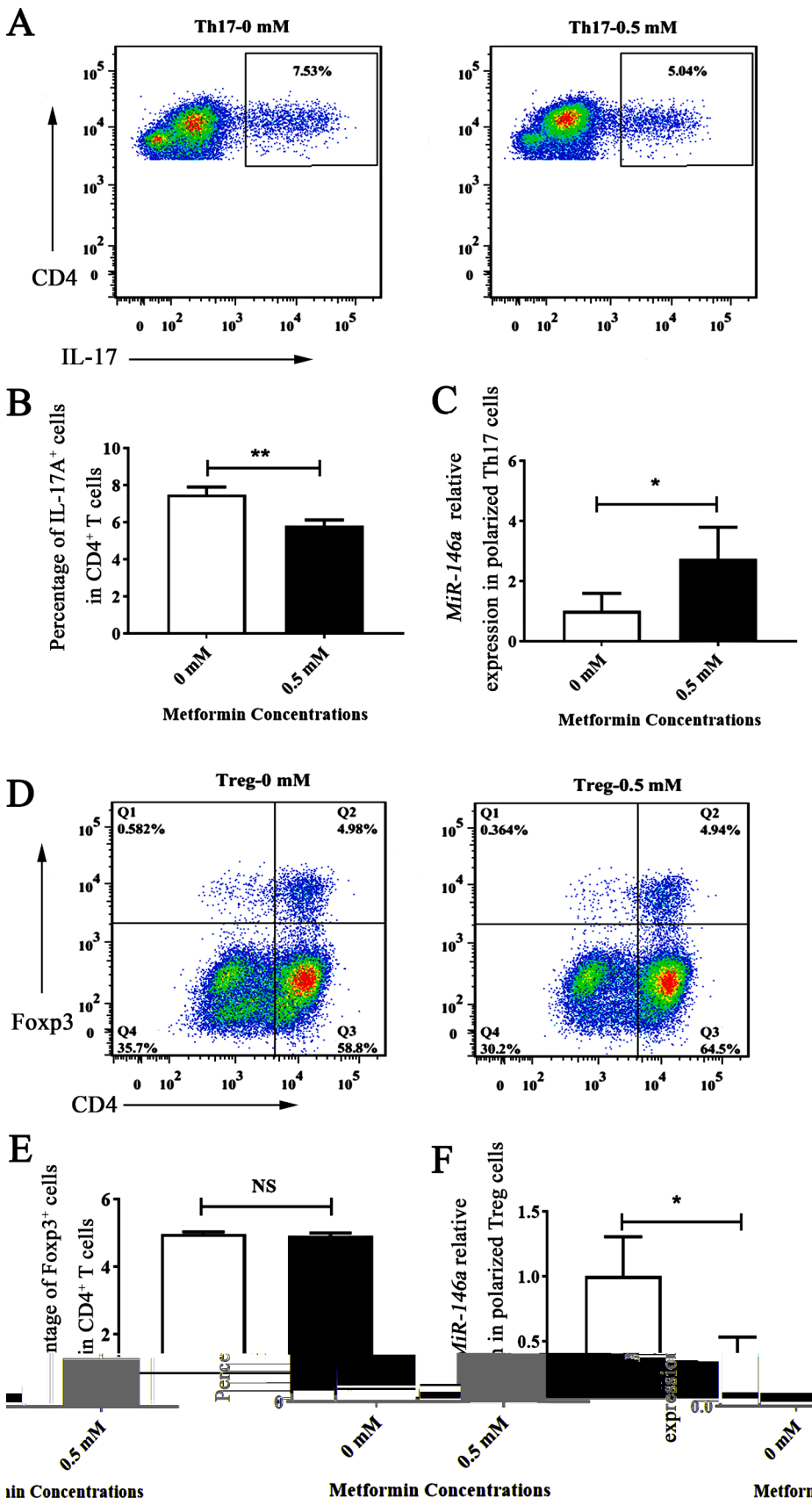


Fig. 6. The influence of metformin on the expression of miR-146a in Th17 and Treg cells. Flow cytometry analysis illustrated the percentages of Th17 cells (A) and Treg cells (D) with or without metformin treatment. (B) Flow cytometry analysis statistics chart for Th17 cells. (C) Expression of miR-146a in Th17 cells. (E) Flow cytometry analysis statistics chart for Treg cells. (F) Expression of miR-146a in Treg cells. Data are presented as the mean \pm SD from two independent experiments with six rats per condition per experiment, * $P < 0.05$, ** $P < 0.01$, t test ($n = 6$).

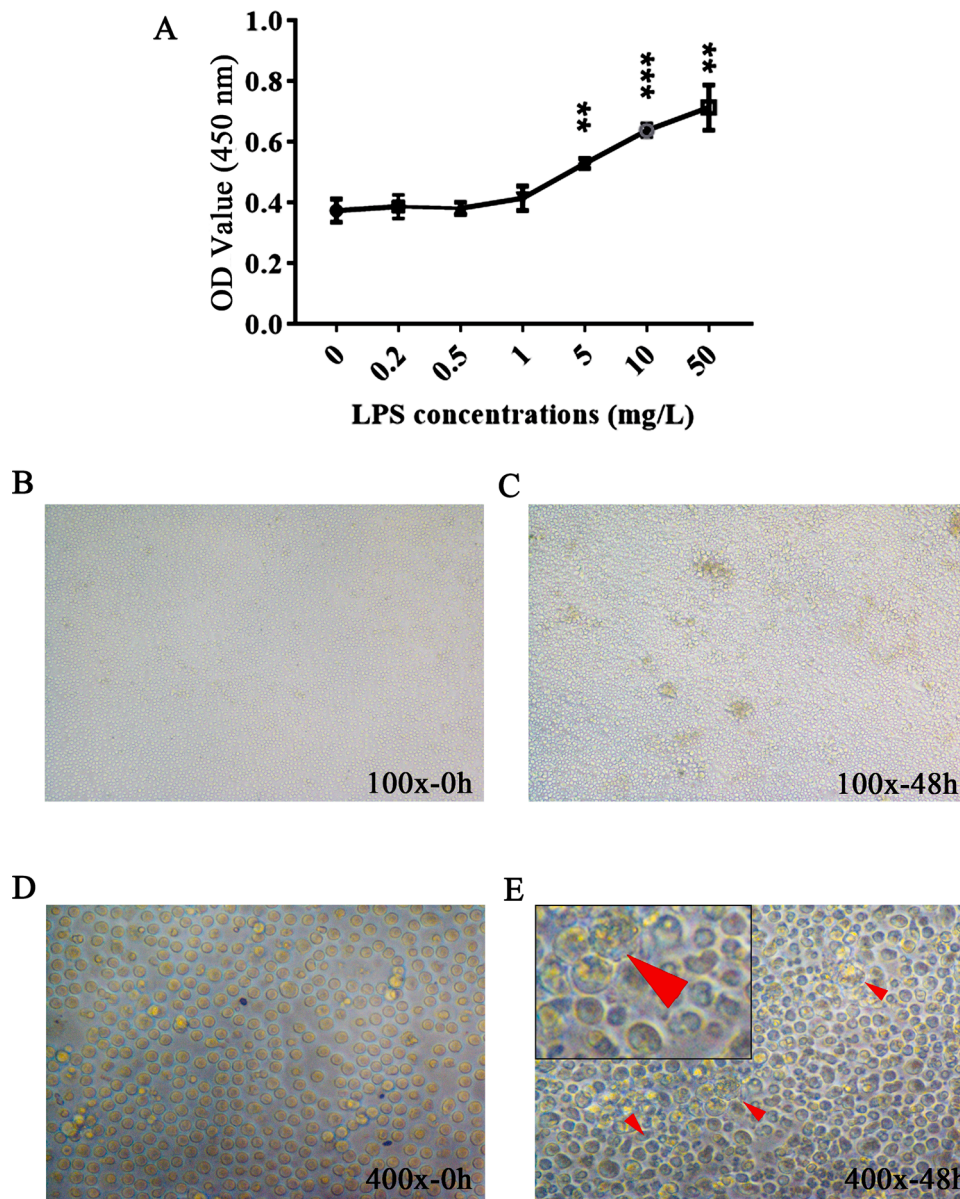


Fig. 7. LPS stimulation *in vitro*. (A) Proliferation assay with a CCK8 kit after stimulation with different doses of LPS. Cell clone formation (B-C) and increased cell volume (D-E) after 0 or 48 h of stimulation. Data are presented as the mean \pm SD from independent experiments with three rats per condition per experiment, ** $P < 0.01$, *** $P < 0.001$, *t* test, arrow represents cells with increased volume ($n = 3$).

mitochondrial function, metabolism, and its anti-inflammatory properties [55]. Metformin can improve arthritis by inhibiting osteoclast formation and reducing osteoclast-specific gene expression in rheumatoid arthritis patients. Metformin can also downregulate the expression of TNF- α -induced genes encoding inflammatory cytokines, proteases, and growth factors in MH7A cells [56]. Furthermore, metformin inhibits the proliferation of fibroblast-like synoviocytes in rheumatoid arthritis via the IGF-IR/PI3K/AKT/mTOR pathway [57]. In the classic animal model of multiple sclerosis, a decrease in microglia and astrocytes, but an increase in oligodendrocytes, was observed after metformin treatment, which improved the steady state of mitochondria through AMPK signals [58].

It has been reported that metformin can remarkably increase miR-146a expression, thus relieving the symptoms of diabetic patients [25]. In addition, metformin can also improve the high-fat-induced endothelial inflammatory response by altering the functions of miR-146a and miR-155 [59]. In our previous studies, we found that metformin can alleviate the development of EAMG disease by inhibiting

the polarization of Th17 cells without limiting that of iTreg cells [27]. Together with this evidence, we hypothesized that metformin might have effects on the development of EAMG by targeting miR-146a.

For *in vitro* assays, the concentrations of metformin were determined by CCK8 proliferation assays and cell apoptosis assays. We found that 0.5 mmol/L metformin could alter the miR-146a content in lymphocytes without affecting lymphocyte proliferation and viability. Additionally, 0.5 mmol/L metformin inhibited IL-17 secretion and promoted miR-146a expression in Th17 cells while inhibiting miR-146a expression in Treg cells, though Foxp3 expression was not affected.

Previous studies have indicated that the imbalance of Th17 and Treg cells is considered to be the main cause of the production of various proinflammatory factors and the release of antibodies in autoimmune diseases. Thus, maintaining the balance between Th17 and Treg cells is key to the treatment of autoimmune diseases [60]. Following metformin treatment, Th17-cell differentiation was clearly inhibited, while Treg differentiation remained unchanged. Therefore, the imbalance between Th17 cells and Treg cells was reversed, which led to the improvement of

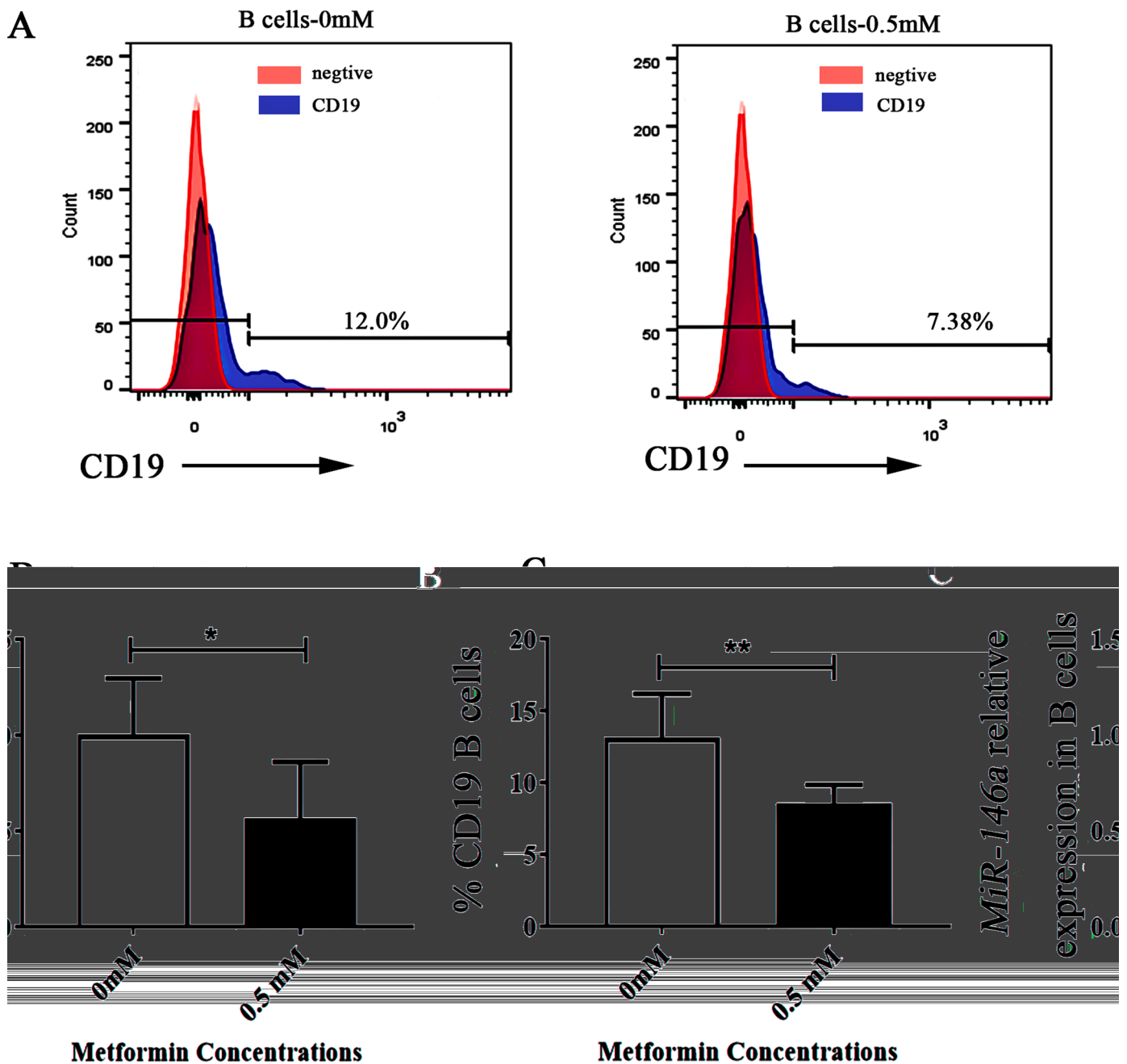


Fig. 8. The influence of metformin on the expression of miR-146a in B cells. (A) Flow cytometry analysis illustrating the percentage of CD19⁺ cells. (B) Flow cytometry analysis statistics chart of CD19⁺ cells. (C) Expression of miR-146a in CD19⁺ B cells. Data are presented as the mean ± SD from independent experiments with five rats per condition per experiment, * $P < 0.05$, ** $P < 0.01$, t test ($n = 5$).

EAMG disease. In addition, our study showed an upregulation of miR-146a levels in EAMG-derived B cells, while 0.5 mmol/L metformin incubation reduced miR-146a expression in EAMG-derived B cells. These data indicate an inhibitory effect of metformin on EAMG-specific B cells and Th17 cells. For this reason, we further explored the effect of metformin on miR-146a in Treg cells, as well as the different target genes of miR-146a in T and B cells.

We first screened target genes of miR-146a using three databases. Among the 20 predicted rno-MiR-146a-5p downstream target genes we screened, the *Irak1*, *Hnrnpd*, *Nova1*, *Btg2*, *Traf6*, *Siah2*, *Brd4*, *Ppp1r11*, *Dot1l* and *Kdm2b* genes are thought to be related to T-cell functions, while the *Irak1*, *Usp3*, *Traf6*, *Siah2*, *Brd4* and *Dot1l* genes are thought to be related to B-cell's (Table 1), and metformin could affect T and B-cell functions by targeting some of these screened genes. Our predicted

downstream target genes provide insight on the regulatory mechanisms by which miR-146a participates in immune responses.

In summary, for the first time, our research group demonstrated diverse expression of miR-146a in an EAMG rat model, showing that it was overexpressed in the spleen and increased significantly in disease-derived B cells, but expressed at low levels in Th17 and Treg cells. Metformin partially inhibited the pathogenicity of AChR-specific B and Th17 cells by targeting miR-146a, and we also predicted the possible downstream target genes of miR-146a in B or T cells. Therefore, miR-146a may serve as a biological marker or a potential therapeutic target of human myasthenia gravis.

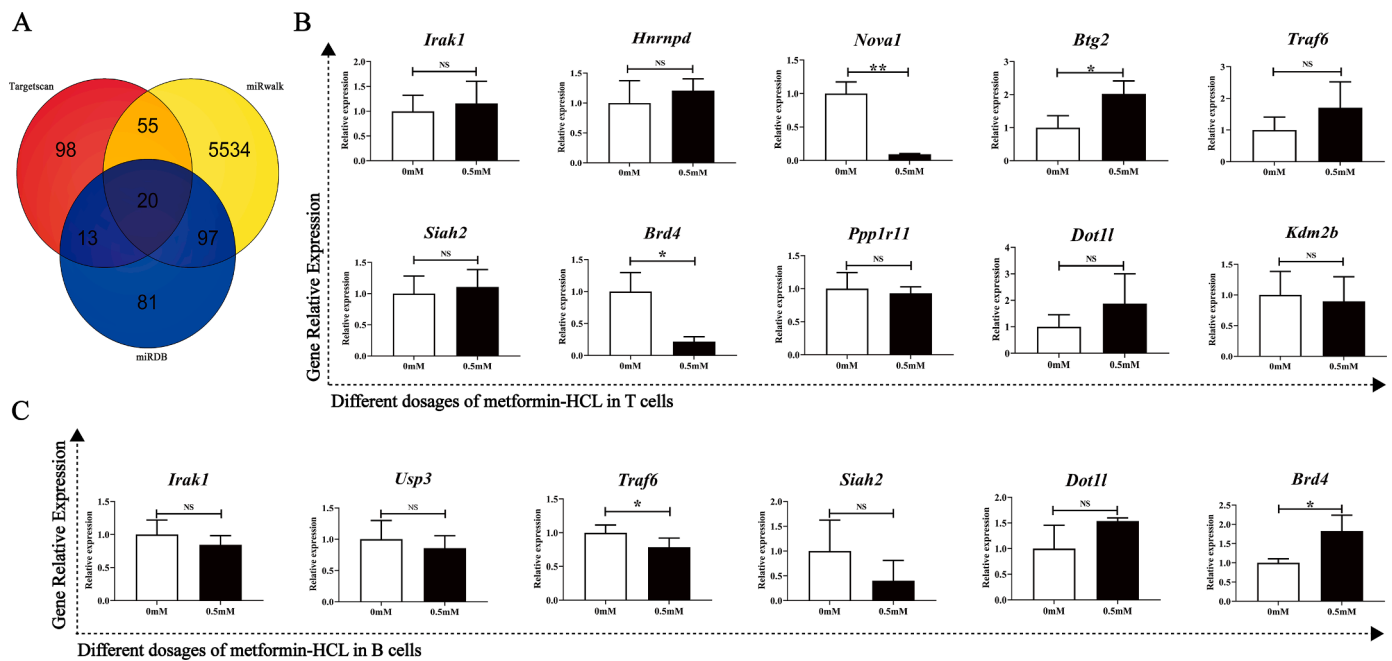


Fig. 9. Prediction and detection of downstream target genes of Rno-miR-146a-5p. (A) Screening of target genes. (B) The influence of metformin on the expression of different target genes (*Irak1*, *Hnrnpd*, *Nova1*, *Btg2*, *Traf6*, *Siah2*, *Brd4*, *Ppp1r11*, *Dot1l* and *Kdm2b*) in T cells compared with the nontreated group. NS = no significant difference, * $P < 0.05$, ** $P < 0.01$, *t* test ($n = 3$). (C) The influence of metformin on the expression of different target genes (*Irak1*, *Usp3*, *Traf6*, *Siah2*, *Brd4* and *Dot1l*) in B cells compared with the nontreated group. NS = no significant difference, * $P < 0.05$, *t* test ($n = 3$).

Table 1

Predicted list of miR-146a downstream target genes associated with T and B-cell functions.

Immune cells	Genes
T cells	<i>Irak1</i> , <i>Hnrnpd</i> , <i>Nova1</i> , <i>Btg2</i> , <i>Traf6</i> , <i>Siah2</i> , <i>Brd4</i> , <i>Ppp1r11</i> , <i>Dot1l</i> , <i>Kdm2b</i>
B cells	<i>Irak1</i> , <i>Usp3</i> , <i>Traf6</i> , <i>Siah2</i> , <i>Brd4</i> , <i>Dot1l</i>

Declaration of Competing Interest

All authors claim that they have no competing interests.

Acknowledgements

Not applicable.

Reference

[1] N.E. Gilhus, G.O. Skeie, F. Romi, K. Lazaridis, P. Zisimopoulou, S. Tzartos, Myasthenia gravis - autoantibody characteristics and their implications for therapy, *Nat. Rev. Neurol.* 12 (5) (2016) 259–268.
 [2] B.M. Conti-Fine, M. Milani, H.J. Kaminski, Myasthenia gravis: past, present, and future, *J. Clin. Invest.* 116 (11) (2006) 2843–2854.
 [3] J.S. Yi, J.T. Guptill, P. Stathopoulos, R.J. Nowak, K.C. O'Connor, B cells in the pathophysiology of myasthenia gravis, *Muscle Nerve* 57 (2) (2018) 172–184.
 [4] R. Hohlfeld, K.V. Toyka, K. Heinger, H. Grosse-Wilde, I. Kalies, Autoimmune human T lymphocytes specific for acetylcholine receptor, *Nature* 310 (5974) (1984) 244–246.
 [5] D.C. Parker, The functions of antigen recognition in T cell-dependent B cell activation, *Semin. Immunol.* 5 (6) (1993) 413–420.
 [6] H. Schaffert, A. Pelz, A. Saxena, M. Losen, A. Meisel, A. Thiel, S. Kohler, IL-17-producing CD4(+) T cells contribute to the loss of B-cell tolerance in experimental autoimmune myasthenia gravis, *Eur. J. Immunol.* 45 (5) (2015) 1339–1347.
 [7] K.M. Danikowski, S. Jayaraman, B.S. Prabhakar, Regulatory T cells in multiple sclerosis and myasthenia gravis, *J. Neuroinflammation* 14 (1) (2017) 117.
 [8] Y. Cao, R.A. Amezquita, S.H. Kleinstein, P. Stathopoulos, R.J. Nowak, K. C. O'Connor, Autoreactive T Cells from Patients with Myasthenia Gravis Are Characterized by Elevated IL-17, IFN-gamma, and GM-CSF and Diminished IL-10 Production, *J. Immunol.* (Baltimore, Md.: 1950) 196 (5) (2016) 2075–2084.
 [9] P. Strobel, M. Helmreich, G. Menioudakis, S.R. Lewin, T. Rudiger, A. Bauer, V. Hoffacker, R. Gold, W. Nix, B. Schalke, O. Elert, M. Semik, H.K. Muller-

Hermelink, A. Marx, Paraneoplastic myasthenia gravis correlates with generation of mature naive CD4(+) T cells in thymomas, *Blood* 100 (1) (2002) 159–166.
 [10] S. Gertel-Lapter, K. Mizrachi, S. Berrih-Aknin, S. Fuchs, M.C. Souroujon, Impairment of regulatory T cells in myasthenia gravis: studies in an experimental model, *Autoimmun Rev.* 12 (9) (2013) 894–903.
 [11] A. Balandina, S. Lecart, P. Darteville, A. Saoudi, S. Berrih-Aknin, Functional defect of regulatory CD4(+)CD25+ T cells in the thymus of patients with autoimmune myasthenia gravis, *Blood* 105 (2) (2005) 735–741.
 [12] Y. Lee, M. Kim, J. Han, K.H. Yeom, S. Lee, S.H. Baek, V.N. Kim, MicroRNA genes are transcribed by RNA polymerase II, *EMBO J.* 23 (20) (2004) 4051–4060.
 [13] M.R. Paterson, A.J. Kriegel, MiR-146a/b: a family with shared seeds and different roots, *Physiol. Genomics* 49 (4) (2017) 243–252.
 [14] B. Li, X. Wang, I.Y. Choi, Y.C. Wang, S. Liu, A.T. Pham, H. Moon, D.J. Smith, D. S. Rao, M.P. Boldin, L. Yang, miR-146a modulates autoreactive Th17 cell differentiation and regulates organ-specific autoimmunity, *J. Clin. Invest.* 127 (10) (2017) 3702–3716.
 [15] K.D. Taganov, M.P. Boldin, K.J. Chang, D. Baltimore, NF-kappaB-dependent induction of microRNA miR-146, an inhibitor targeted to signaling proteins of innate immune responses, *Proc. Natl. Acad. Sci. U S A* 103 (33) (2006) 12481–12486.
 [16] M.P. Boldin, K.D. Taganov, D.S. Rao, L. Yang, J.L. Zhao, M. Kalwani, Y. Garcia-Flores, M. Luong, A. Devrekanli, J. Xu, G. Sun, J. Tay, P.S. Linsley, D. Baltimore, miR-146a is a significant brake on autoimmunity, myeloproliferation, and cancer in mice, *J. Exp. Med.* 208 (6) (2011) 1189–1201.
 [17] J.L. Zhao, D.S. Rao, M.P. Boldin, K.D. Taganov, R.M. O'Connell, D. Baltimore, NF-kappaB dysregulation in microRNA-146a-deficient mice drives the development of myeloid malignancies, *Proc. Natl. Acad. Sci. U S A* 108 (22) (2011) 9184–9189.
 [18] R. Liu, B. Yi, S. Wei, W.H. Yang, K.M. Hart, P. Chauhan, W. Zhang, X. Mao, X. Liu, C.G. Liu, L. Wang, FOXP3-miR-146-NF-kappaB axis and therapy for precancerous lesions in prostate, *Cancer Res.* 75 (8) (2015) 1714–1724.
 [19] A. Srivastava, P. Nikamo, W. Lohcharenkal, D. Li, F. Meisgen, N. Xu Landen, M. Stahle, A. Pivarcsi, E. Sonkoly, MicroRNA-146a suppresses IL-17-mediated skin inflammation and is genetically associated with psoriasis, *J. Allergy Clin. Immunol.* 139 (2) (2017) 550–561.
 [20] J. Zhang, G. Jia, Q. Liu, J. Hu, M. Yan, B. Yang, H. Yang, W. Zhou, J. Li, Silencing miR-146a influences B cells and ameliorates experimental autoimmune myasthenia gravis, *Immunology* 144 (1) (2015) 56–67.
 [21] E. Tuzun, S. Berrih-Aknin, T. Brenner, L.L. Kusner, R. Le Panse, H. Yang, S. Tzartos, P. Christodoss, Guidelines for standard preclinical experiments in the mouse model of myasthenia gravis induced by acetylcholine receptor immunization, *Exp. Neurol.* 270 (2015) 11–17.
 [22] M. Losen, P. Martinez-Martinez, P.C. Molenaar, K. Lazaridis, S. Tzartos, T. Brenner, R.S. Duan, J. Luo, J. Lindstrom, L. Kusner, Standardization of the experimental autoimmune myasthenia gravis (EAMG) model by immunization of rats with Torpedo californica acetylcholine receptors—Recommendations for methods and experimental designs, *Exp. Neurol.* 270 (2015) 18–28.
 [23] L.P. Bharath, M. Agrawal, G. McCambridge, D.A. Nicholas, H. Hasturk, J. Liu, K. Jiang, R. Liu, Z. Guo, J. Deeney, C.M. Apovian, J. Snyder-Cappione, G.S. Hawk-

- R.M. Fleeman, R.M.F. Pihl, K. Thompson, A.C. Belkina, L. Cui, E.A. Proctor, P. A. Kern, B.S. Nikolajczyk, Metformin enhances autophagy and normalizes mitochondrial function to alleviate aging-associated inflammation, *Cell Metab.* 32 (1) (2020) 44–55, e6.
- [24] Y. Jing, F. Wu, D. Li, L. Yang, Q. Li, R. Li, Metformin improves obesity-associated inflammation by altering macrophages polarization, *Mol. Cell Endocrinol.* 461 (2018) 256–264.
- [25] E. Mensa, A. Giuliani, G. Maccacchione, F. Gurau, A.R. Bonfigli, F. Romagnoli, M. De Luca, J. Sabbatinelli, F. Olivieri, Circulating miR-146a in healthy aging and type 2 diabetes: Age- and gender-specific trajectories, *Mech. Ageing Dev.* 180 (2019) 1–10.
- [26] G. Kanigur Sultuybek, T. Soydas, G. Yenmis, NF-kappaB as the mediator of metformin's effect on ageing and ageing-related diseases, *Clin. Exp. Pharmacol. Physiol.* 46 (5) (2019) 413–422.
- [27] Y. Cui, L. Chang, C. Wang, X. Han, L. Mu, Y. Hao, C. Liu, J. Zhao, T. Zhang, H. Zhang, Y. Zhang, Y. Liu, W. Zhao, J. Wang, X. Liu, B. Sun, G. Wang, Q. Kong, J. Han, H. Li, Metformin attenuates autoimmune disease of the neuromotor system in animal models of myasthenia gravis, *Int. Immunopharmacol.* 75 (2019), 105822.
- [28] S. Duan, F. Wang, J. Cao, C. Wang, Exosomes derived from MicroRNA-146a-5p-enriched bone marrow mesenchymal stem cells alleviate intracerebral hemorrhage by inhibiting neuronal apoptosis and microglial M1 polarization, *Drug Des. Dev. Ther.* 14 (2020) 3143–3158.
- [29] M. Inoue, T. Arikawa, Y.H. Chen, Y. Moriwaki, M. Price, M. Brown, J.R. Perfect, M. L. Shinohara, T cells down-regulate macrophage TNF production by IRAK1-mediated IL-10 expression and control innate hyperinflammation, *Proc. Natl. Acad. Sci. U S A* 111 (14) (2014) 5295–5300.
- [30] P. Zhao, M.M. Ji, Y. Fang, X. Li, H.M. Yi, Z.X. Yan, S. Cheng, P.P. Xu, A. Janin, C. F. Wang, L. Wang, W.L. Zhao, A novel lncRNA TCL1nc1 promotes peripheral T cell lymphoma progression through acting as a modular scaffold of HNRNP and YBX1 complexes, *Cell Death Dis.* 12 (4) (2021) 321.
- [31] S.O. Yoon, E.K. Kim, M. Lee, W.Y. Jung, H. Lee, Y. Kang, Y.J. Jang, S.W. Hong, S. H. Choi, W.I. Yang, NOVA1 inhibition by miR-146b-5p in the remnant tissue microenvironment defines occult residual disease after gastric cancer removal, *Oncotarget* 7 (3) (2016) 2475–2495.
- [32] R. Terra, H. Luo, X. Qiao, J. Wu, Tissue-specific expression of B-cell translocation gene 2 (BTG2) and its function in T-cell immune responses in a transgenic mouse model, *Int. Immunol.* 20 (3) (2008) 317–326.
- [33] X. Ni, W. Kou, J. Gu, P. Wei, X. Wu, H. Peng, J. Tao, W. Yan, X. Yang, A. Lebid, B. V. Park, Z. Chen, Y. Tian, J. Fu, S. Newman, X. Wang, H. Shen, B. Li, B.R. Blazar, X. Wang, J. Barbi, F. Pan, L. Lu, TRAF6 directs FOXP3 localization and facilitates regulatory T-cell function through K63-linked ubiquitination, *EMBO J.* 38 (9) (2019).
- [34] N. Stöckel, G. Prinz, D. Pfeifer, P. Hasselblatt, A. Schmitt-Graeff, M. Follo, R. Thimme, J. Finke, J. Duyster, U. Salzer, R. Zeiser, MiR-146a regulates the TRAF6/TNF-axis in donor T cells during GVHD, *Blood* 124 (16) (2014) 2586–2595.
- [35] H. Chen, N. Wang, G. Yang, Y. Guo, Y. Shen, X. Wang, P. Zhang, Y. Xu, The expression and function of E3 ligase SIAH2 in acute T lymphoblastic leukemia, *Leuk. Res.* 42 (2016) 28–36.
- [36] W. Zhang, C. Prakash, C. Sum, Y. Gong, Y. Li, J.J. Kwok, N. Thiessen, S. Pettersson, S.J. Jones, S. Knapp, H. Yang, K.C. Chin, Bromodomain-containing protein 4 (BRD4) regulates RNA polymerase II serine 2 phosphorylation in human CD4+ T cells, *J. Biol. Chem.* 287 (51) (2012) 43137–43155.
- [37] R.N. Joshi, S.J. Fernandes, M.M. Shang, N.A. Kiani, D. Gomez-Cabrero, J. Tegner, A. Schmidt, Phosphatase inhibitor PPP1R11 modulates resistance of human T cells toward Treg-mediated suppression of cytokine expression, *J. Leukoc. Biol.* 106 (2) (2019) 413–430.
- [38] Y. Kagoya, M. Nakatsugawa, K. Saso, T. Guo, M. Anczurowski, C.H. Wang, M. O. Butler, C.H. Arrowsmith, N. Hirano, DOT1L inhibition attenuates graft-versus-host disease by allogeneic T cells in adoptive immunotherapy models, *Nat. Commun.* 9 (1) (2018) 1915.
- [39] J.A. Kotov, D.I. Kotov, J.L. Linehan, V.J. Bardwell, M.D. Gearhart, M.K. Jenkins, BCL6 corepressor contributes to Th17 cell formation by inhibiting Th17 fate suppressors, *J. Exp. Med.* 216 (6) (2019) 1450–1464.
- [40] R. Chandra, S. Federici, Z.H. Nemeth, B. Csoka, J.A. Thomas, R. Donnelly, Z. Spolarics, Cellular mosaicism for X-linked polymorphisms and IRAK1 expression presents a distinct phenotype and improves survival following sepsis, *J. Leukoc. Biol.* 95 (3) (2014) 497–507.
- [41] I. Cleyneen, E. Vazeille, M. Artieda, H.W. Verspaget, M. Szczypiorska, M.A. Bringer, P.L. Lakatos, F. Seibold, K. Parnell, R.K. Weersma, J.M. Mahachie John, R. Morgan-Walsh, D. Staelens, I. Arijis, G. De Hertogh, S. Muller, A. Tordai, D.W. Hommes, T. Ahmad, C. Wijmenga, S. Pender, P. Rutgeerts, K. Van Steen, D. Lottaz, S. Vermeire, A. Darfeuille-Michaud, Genetic and microbial factors modulating the ubiquitin proteasome system in inflammatory bowel disease, *Gut* 63 (8) (2014) 1265–1274.
- [42] S. Nataf, M. Guillen, L. Pays, Common neurodegeneration-associated proteins are physiologically expressed by human B lymphocytes and are interconnected via the inflammation/autophagy-related proteins TRAF6 and SQSTM1, *Front. Immunol.* 10 (2019) 2704.
- [43] J. Boehm, Y. He, A. Greiner, L. Staudt, T. Wirth, Regulation of BOB.1/OBF.1 stability by SIAH, *EMBO J.* 20 (15) (2001) 4153–4162.
- [44] I.Y. Kong, J.S. Rimes, A. Light, I. Todorovski, S. Jones, E. Morand, D.A. Knight, Y. E. Bergman, S.J. Hogg, H. Falk, B.J. Monahan, P.A. Stuppel, I.P. Street, S. Heinzel, P. Bouillet, R.W. Johnstone, P.D. Hodgkin, S.J. Vervoort, E.D. Hawkins, Temporal analysis of Brd4 displacement in the control of B cell survival, proliferation, and differentiation, *Cell Rep.* 33 (3) (2020), 108290.
- [45] M.A. Aslam, M.F. Alemdehy, E.M. Kwesi-Maliepaard, F.I. Muhaimin, M. Caganova, I.N. Pardieck, T. van den Brand, T. van Welsem, I. de Rink, J.Y. Song, E. de Wit, R. Arens, H. Jacobs, F. van Leeuwen, Histone methyltransferase DOT1L controls state-specific identity during B cell differentiation, *EMBO Rep.* 22 (2) (2021) e51184.
- [46] M. Bhaskaran, M. Mohan, MicroRNAs: history, biogenesis, and their evolving role in animal development and disease, *Vet Pathol.* 51 (4) (2014) 759–774.
- [47] C. Zhou, L. Zhao, K. Wang, Q. Qi, M. Wang, L. Yang, P. Sun, H. Mu, MicroRNA-146a inhibits NF-kappaB activation and pro-inflammatory cytokine production by regulating IRAK1 expression in THP-1 cells, *Exp. Ther. Med.* 18 (4) (2019) 3078–3084.
- [48] J. Li, Y. Wan, Q. Guo, L. Zou, J. Zhang, Y. Fang, J. Zhang, J. Zhang, X. Fu, H. Liu, L. Lu, Y. Wu, Altered microRNA expression profile with miR-146a upregulation in CD4+ T cells from patients with rheumatoid arthritis, *Arthritis Res. Ther.* 12 (3) (2010) R81.
- [49] P.R. Dominguez-Gutierrez, A. Ceribelli, M. Satoh, E.S. Sobel, W.H. Reeves, E. K. Chan, Positive correlation of STAT1 and miR-146a with anemia in patients with systemic lupus erythematosus, *J. Clin. Immunol.* 34 (2) (2014) 171–180.
- [50] N.S. Lai, H.C. Yu, C.H. Tung, K.Y. Huang, H.B. Huang, M.C. Lu, The role of aberrant expression of T cell miRNAs affected by TNF-alpha in the immunopathogenesis of rheumatoid arthritis, *Arthritis Res. Ther.* 19 (1) (2017) 261.
- [51] M. Ammari, J. Presumey, C. Ponsolles, G. Roussignon, C. Roubert, V. Escriou, K. Toupet, A.L. Mausset-Bonnefont, M. Cren, M. Robin, P. Georget, R. Nehmar, L. Taams, J. Grun, A. Grutzkau, T. Haupl, Y.M. Pers, C. Jorgensen, I. Duroux-Richard, G. Courties, F. Apparailly, Delivery of miR-146a to Ly6C(high) Monocytes Inhibits Pathogenic Bone Erosion in Inflammatory Arthritis, *Theranostics* 8 (21) (2018) 5972–5985.
- [52] R.L. Ruff, R.P. Lisak, Nature and action of antibodies in myasthenia gravis, *Neurol. Clin.* 36 (2) (2018) 275–291.
- [53] S. Crotty, A brief history of T cell help to B cells, *Nat. Rev. Immunol.* 15 (3) (2015) 185–189.
- [54] G.X. Zhang, B.G. Xiao, M. Bakhiet, P. van der Meide, H. Wigzell, H. Link, T. Olsson, Both CD4+ and CD8+ T cells are essential to induce experimental autoimmune myasthenia gravis, *J. Exp. Med.* 184 (2) (1996) 349–356.
- [55] Y. Saisho, Metformin and inflammation: its potential beyond glucose-lowering effect, *Endocr. Metab. Immune Disord. Drug Targets* 15 (3) (2015) 196–205.
- [56] Y. Matsuoka, S. Morimoto, M. Fujishiro, K. Hayakawa, Y. Kataoka, S. Suzuki, K. Ikeda, K. Takamori, K. Yamaji, N. Tamura, Metformin repositioning in rheumatoid arthritis, *Clin. Exp. Rheumatol.* 39 (4) (2021) 763–768.
- [57] K. Chen, Z.W. Lin, S.M. He, C.Q. Wang, J.C. Yang, Y. Lu, X.B. Xie, Q. Li, Metformin inhibits the proliferation of rheumatoid arthritis fibroblast-like synoviocytes through IGF-IR/PI3K/AKT/m-TOR pathway, *Biomed. Pharmacother.* 115 (2019), 108875.
- [58] S.H.H. Lergani, M. Borhani-Haghighi, P. Pasbakhsh, V.P. Mahabadi, S. Nekoonam, E. Shiri, I.R. Kashani, A. Zendehtdel, Oligoprotective effect of metformin through the AMPK-dependent on restoration of mitochondrial hemostasis in the cuprizone-induced multiple sclerosis model, *J. Mol. Histol.* 50 (3) (2019) 263–271.
- [59] L. Gou, G. Liu, R. Ma, A. Regmi, T. Zeng, J. Zheng, X. Zhong, L. Chen, High fat-induced inflammation in vascular endothelium can be improved by *Abelmoschus esculentus* and metformin via increasing the expressions of miR-146a and miR-155, *Nutr. Metab. (Lond)* 17 (2020) 35.
- [60] A. Uzawa, N. Kawaguchi, K. Himuro, T. Kanai, S. Kuwabara, Serum cytokine and chemokine profiles in patients with myasthenia gravis, *Clin. Exp. Immunol.* 176 (2) (2014) 232–237.